Neurobiology of Disease 124 (2019) 108–117

Contents lists available at ScienceDirect

Neurobiology of Disease

journal homepage: www.elsevier.com/locate/ynbdi

Astrocytic expression of the chaperone DNAJB6 results in non-cell autonomous protection in Huntington's disease

Matteo Bason, Melanie Meister-Broekema, Niels Alberts, Pascale Dijkers, Steven Bergink, Ody C.M. Sibon, Harm H. Kampinga*

Department of Cell Biology, UMCG and University of Groningen, Ant. Deusinglaan 1, Groningen 9713AV, the Netherlands

ARTICLE INFO

Keywords:
Neurodegeneration
Polyglutamine
Aggregation
Astrocytes
Chaperones
DNAJB6
Prion-like aggregate spreading

ABSTRACT

Several neurodegenerative diseases like Huntington's, a polyglutamine (PolyQ) disease, are initiated by protein aggregation in neurons. Furthermore, these diseases are also associated with a multitude of responses in non-neuronal cells in the brain, in particular glial cells, like astrocytes. These non-neuronal responses have repeatedly been suggested to play a disease-modulating role, but how these may be exploited to delay the progression of neurodegeneration has remained unclear. Interestingly, one of the molecular changes that astrocytes undergo includes the upregulation of certain Heat Shock Proteins (HSPs) that are classically considered to maintain protein homeostasis, thus resulting in cell autonomous protection. Previously, we discovered DNAJB6, a member of the human DNAJ family, as potent cell autonomous suppressor of PolyQ aggregation and related neurodegeneration. Using cell type specific expression systems in *D. melanogaster*, we show that exclusive expression of DNAJB6 in astrocytes (that do not express PolyQ protein) can delay neurodegeneration and expands lifespan when the PolyQ protein is exclusively expressed in neurons (that do not co-express DNAJB6 themselves). This provides direct evidence for a non-cell autonomous protective role of astrocytes in PolyQ diseases.

1. Introduction

Heat Shock Proteins (HSPs) are key regulators of the cellular protein quality control (PQC) system (Hartl et al., 2011). In addition to their roles in protein folding, protein transport and protein complex remodelling, HSPs have also been implied in the disaggregation, as well as in the degradation of un- or misfolded proteins (Kakkar et al., 2014). Many age-related neurodegenerative diseases (NDs) are characterized by protein aggregates in neurons and these are thought to initiate or drive their pathology and degeneration (Kakkar et al., 2014; Kampinga and Bergink, 2016).

These findings have led to the speculation that an age-related decline in PQC may be key to disease initiation (Balch et al., 2008) and also suggested that boosting the (selective) activity of components of the cellular PQC such as HSPs may hold promises for counteracting NDs (Kakkar et al., 2014; Kampinga and Bergink, 2016; Balch et al., 2008). In line with these hypotheses, we and others have performed several forward genetic screens to identify specific HSPs within the PQC network that may serve to prevent the aggregation of disease-related proteins and thereby delay the onset of NDs (Hageman et al., 2011; Vos et al., 2010; Hageman et al., 2010; Kakkar et al., 2016a). In such screens, we identified DNAJB6, a human HSP of the DNAJ family and HSP70 co-chaperone, as a very potent and cell autonomous inhibitor of protein aggregation in different in vitro and in vivo models of PolyQ diseases (Hageman et al., 2011; Kakkar et al., 2016b), including Huntington's disease (HD, OMIM:#143100), which is characterized by the aggregation of mutant PolyQ Huntingtin (HTT). DNAJB6 is a ubiquitously expressed and non-stress-regulated co-chaperone of HSP70 that forms highly dynamic oligomers (Hageman et al., 2011; Kakkar et al., 2016b). It can bind to early intermediates (but not to monomers) of PolyQ containing peptides that initiate fibril formation via direct interaction to the amyloidogenic core (i.e. the polyQ sequence) of polyglutamine containing protein fibrils, thus potently preventing primary nucleation and (to a lesser extent) also secondary nucleation (Kakkar et al., 2016b; Gillis et al., 2013; Månsson et al., 2014). DNAJB6 differs from other HSPs (such as HSP70 and DNAJB1) that cannot suppress aggregation by the core PolyQ peptide, although they can act on sequences flanking the amyloidogenic PolyQ core (Hageman et al., 2011;

Abbreviations: ATXN3, ataxin-3; HMW, high molecular weight; HSPs, Heat Shock Proteins; HD, Huntington's disease; HTT, Huntingtin; PolyQ, Polyglutamine; PQC, protein quality control; NDs, neurodegenerative diseases.

* Corresponding author.
E-mail address: h.h.kampinga@umcg.nl (H.H. Kampinga).

https://doi.org/10.1016/j.nbd.2018.10.017
Received 11 August 2018; Received in revised form 2 October 2018; Accepted 28 October 2018
Available online 05 November 2018

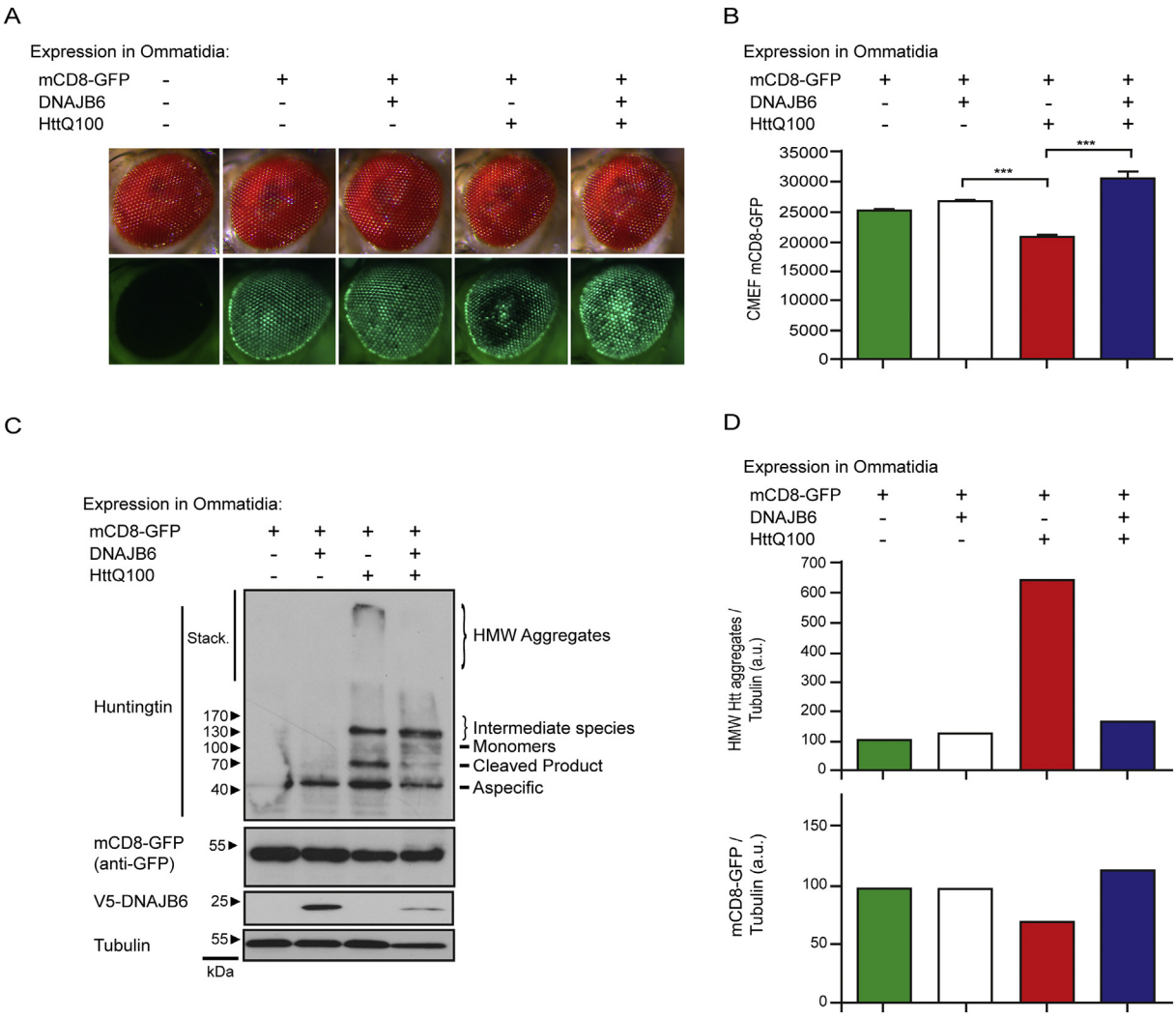

Fig. 1. Protective activity of DNAJB6 against PolyQ-HTT-mediated degeneration in *D. melanogaster* ommatidia. **A)** Representative images of eyes in 48 h old adult male flies expressing the indicated transgenes in ommatidia. mCD8-GFP is a reporter for ommatidia integrity. Genotypes in Materials and Methods. **B)** Quantification of the corrected mean eye fluorescence (CMEF) for mCD8-GFP of Fig. 1A. Statistical significance was analysed using 10 eyes/group with 1-way ANOVA test (SEM, ***, $p < 0.001$). **C)** Western Blots of total head lysates of 48 h old adult female flies expressing the indicated transgenes in ommatidia. Anti-huntingtin antibody used for detection of monomers (100 kDa), cleaved products (70 kDa), intermediate aggregated species (130–170 kDa) and HMW aggregates (stacking gel) of HttQ100-mRFP. Anti-GFP antibody used for mCD8-GFP detection. Anti-V5 antibody for (V5 tagged) DNAJB6 detection. Tubulin was used as loading control. Number of fly heads per each lysate sample and genotypes in Materials and Methods. **D)** Quantification of HMW aggregates of HttQ100-mRFP (signal in stacking gel) and mCD8-GFP of data of Fig. 1C (signal normalized on tubulin; a.u.: arbitrary units).

Månsson et al., 2014). In line, DNAJB6 has been shown to inhibit aggregation not only of PolyQ HTT, but also of PolyQ ATXN3 and PolyQ androgen receptor (Hageman et al., 2010). This specific function of DNAJB6 is dependent on a unique S/T-rich region in DNAJB6, which is exposed on the DNAJB6 surface and where the amyloid-forming peptides can bind (Kakkar et al., 2016b; Söderberg et al., 2018; Månsson et al., 2018). In addition to protein aggregation, a common hallmark of nearly all aggregation-related NDs is the reactivity of astrocytes, a specific type of glial cells that normally contributes to the brain homeostasis and supports the neuronal functions (Sofroniew and Vinters, 2010). The astrocytic response during aggregation-related NDs is found in degenerating areas of the brain and is characterized by a spectrum of progressive molecular, cellular and functional changes (Sofroniew and Vinters, 2010; Ben Haim et al., 2015), which are most likely a response triggered by the neuronal damage. On one hand, the (early) astrocytic response has repeatedly been suggested to serve in a protective manner to counteract the progression of neurodegeneration. On the other hand, (chronic) astrocytic reactivity has also been suggested to be a maladaptive response that leads to disease aggravation (Sofroniew, 2009).

Interestingly, one of the molecular changes detected in astrocytes in human brains affected by neurodegeneration includes the up-regulation of certain HSPs (Durrenberger et al., 2009; Seidel et al., 2012; Wilhelmus et al., 2006; Dabir et al., 2004), including DNAJB6 (Durrenberger et al., 2009). However, the functional implications of HSPs-up-regulations for the progression of neuronal degeneration have not yet been established.

To fully explore whether and how the expression of HSPs contributes to neuroprotection in NDs, we generated *D.melanogaster* models that exclusively express PolyQ-HTT in neurons, whilst co-expressing human DNAJB6 either in the same neurons (to study cell autonomous effects) or in astrocytes (to study non-cell autonomous effects).

Our studies show that human DNAJB6 can provide cell autonomous protection against PolyQ mediated neurodegeneration in *D.melanogaster*, which is associated with a reduction in the PolyQ-HTT aggregate load in fly brains. Strikingly, the exclusive expression of DNAJB6 in astrocytes also provides non-cell autonomous protection against progressive neuronal degeneration and prolongs organismal

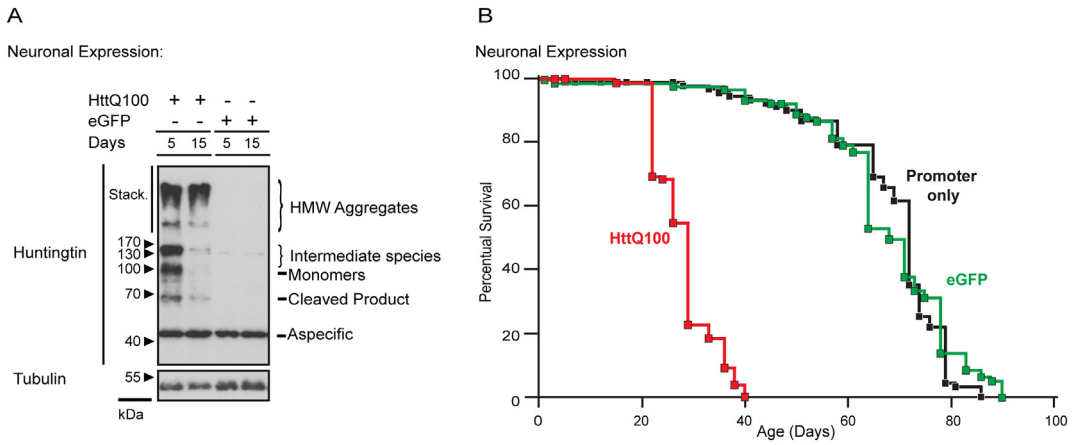

Fig. 2. Pan-Neuronal expression of PolyQ-HTT causes aggregate formation and reduces lifespan in *D. melanogaster*. A) Western Blots of total head lysates of 5 and 15-day-old adult male flies expressing the indicated transgenes in all neurons. Anti-huntingtin antibody for detection of monomers (100 kDa), cleaved products (70 kDa), intermediate aggregated species (130–170 kDa) and HMW aggregates (stacking gel) of HttQ100-mRFP. Tubulin was used as loading control. Number of fly heads per each lysate sample and genotypes in Materials and Methods. **B)** Lifespan of the same isogenised males flies expressing HttQ100-mRFP or control transgene (eGFP or only promoter) in all neurons. Lifespan of HttQ100-mRFP-expressing line (red curve) is significantly reduced compared to the eGFP-expressing control line (green curve). Detailed statistics, comparisons and genotypes are provided in Fig. S2-1B. (For interpretation of the references to colour in this figure legend, the reader is referred to the web version of this article.)

lifespan, although not accompanied by a reduction in the PolyQ-HTT aggregate load in the fly brains. Rather, under these conditions, in flies that express DNAJB6 in astrocytes, a high fraction of astrocytes now contain neuronal derived PolyQ-HTT aggregates, in line with the suggestion that astrocytes might take up prion-like PolyQ-HTT aggregates species, a capacity that is enhanced by DNAJB6 expression (Brundin et al., 2010; Costanzo and Zurzolo, 2013; Ren et al., 2009; Babcock and Ganetzky, 2015).

2. Materials and methods

2.1. Vectors

UAS/LexO vectors were obtained by cloning the sequences of HttQ100-mRFP (Prof. T. Littleton Group, MIT) or V5-DNAJB6 (isoform B) or eGFP (Clontech) in the multiple cloning site of pUAS *attB* or pLexO *attB* (Prof. K. Basler Group, UZH). Driver (Promoter cell-specific expression) vectors were obtained starting from the backbone of plasmids pDPP-Gal4 *attB* or pDPP-LG *attB* or pDPP-LhG *attB* (Prof. K. Basler Group, UZH). DPP promoter was substituted with the sequence of promoter *elav* (pan-neuronal, from p*Elav*-Casper vector, Prof. Liqun Luo, Stanford University), *repo* (pan-glial, from pENTRY-D-TOPO-*Repo*4.3 vector, Prof. C. Klämbt, University of Münster) or *alrm* (astrocytic, from p*Alrm*-Casper vector, Prof. M. Freeman, UMASS). All obtained vectors were sequenced. See Table T1 for vectors list.

2.2. D. melanogaster stocks

The *D. melanogaster* lines of Table T1 were obtained by injection and transformation of embryos with the above mentioned *attB* vectors, based on *attP*-site specific PhiC31 integrase system, by Best Gene Inc. injection service. *D. melanogaster* lines from Bloomington Drosophila Stock Center were also used: *gmr-Gal4* (Line BDSC #8121 in Fig. 1); *gmr-Gal4* (Line BDSC #1104 in Fig. S1-1); *alrm-Gal4* (Line BDSC #67031 in Fig. S1-1); UAS-mCD8-GFP (Line BDSC #5130); UAS-mCD8-RFP (Line BDSC #27391); UAS-ATXN3-Q78 (Line BDSC #8150 in Fig. S1-1); *gmr-QF2* (Line BDSC #59283 in Fig. S1-1 was a gift from C. Potter, Baltimore, MD, U.S.A.). *gmr-QF2* and QUAS-ATXN3-Q78 are based on the Q expression system in *D.melanogaster* (Potter et al., 2010). All the lines were isogenised to remove background mutations by backcrossing each of them for 6 generations with the control stock w^{1118} line.

2.3. Genotypes

Fig. 1: *w(−); UAS HttQ100-mRFP / + (or UAS DNAJB6); gmr Gal4 / UAS mCD8-GFP (or +)*. Fig. S1-1: for cell-autonomous rescue: *w(−); gmr-Gal4:UAS ATXN3-Q78/ UAS DNAJB6 (or +); +/+*. For non-cell autonomous rescue: *w(−),gmr-QF2; alrm-Gal4:QUAS ATXN3-Q78/ UAS DNAJB6 (or +); +/+*. Fig. 2A, S2-1A: *w(−); UAS HttQ100-mRFP (or UAS eGFP) / +; elav Gal4/+*. Fig. 3B and S3-1H: 1) Control line (red): *w(−); UAS HttQ100-mRFP / elav LhG; elav Gal4 / LexO eGFP*. 2) Rescued line (blue): *w(−); UAS HttQ100-mRFP / elav LhG; elav Gal4 / LexO DNAJB6*. Fig. S3-1B: 1) active combinations *w(−); UAS eGFP (D) /+; promoter Gal4/+*. 2) inactive combinations: *w(−); UAS eGFP/ promoter LexA; +/+ or w(−); promoter Gal4/+; LexO eGFP (A) /+*. Fig. S3-1C: *w(−); UAS eGFP/+; promoter Gal4/+ or w(−);promoter LexA (LG or LhG)/+; LexO eGFP/+*. Negative control: *w(−);+/+;+/+*. Fig. S3-1D: *w(−); UAS eGFP(D)/+; promoter Gal4/+ or w(−);promoter LexA (LG or LhG)/+; LexO eGFP(A)/+*. Negative control: *w(−);+/+;+/+*. Fig. 4A and B*: w(−); UAS mCD8-RFP(or UAS HttQ100-mRFP) / alrm LhG; elav Gal4 / LexO eGFP*. Fig. 5A and Fig. S5-1B: 1) control line (red): *w(−); UAS HttQ100-mRFP / promoter(repo* or *alrm) LhG; elav Gal4 / LexO eGFP*. 2) Rescued line (blue): *w(−); UAS HttQ100-mRFP / promoter (repo* or *alrm) LhG; elav Gal4 / LexO DNAJB6*. Fig. 5B and Fig. S5-1E: 1) Control (Fig. 5B, panel 1 and Fig. S5-1E, panels 1–3): *w(−); UAS CD8-mRFP / alrm LhG; elav Gal4 / LexO eGFP*. 2) Condition 1 (Fig. 5B, panel 2 and Fig. S5-1E, panels 4–6): *w(−); UAS HttQ100-mRFP / alrm LhG; elav Gal4 / LexO eGFP*. 3) Condition 2 (Fig. 5B, panel 3 and Fig. S5-1E, panels 7–9; Fig. 5C and Supplementary Movie M1): *w(−); UAS HttQ100-mRFP / alrm LhG; elav Gal4 / LexO DNAJB6*. Fig. 5E and Fig. S5-1H: 1) Control line (red): *w(−); UAS HttQ100-mRFP / promoter (elav or alrm) LhG; elav Gal4 / LexO eGFP*. 2) Rescued line (blue): *w(−); UAS HttQ100-mRFP / promoter (elav or alrm) LhG; elav Gal4 / LexO DNAJB6*. Fig. S5-1F: *w(−); UAS HttQ100-mRFP (or +) / +; elav Gal4/+*.

2.4. Antibodies and reagents

Antibodies (dilutions are indicated in brackets for western blots (WB) and immunofluorescence (IF)) against huntingtin (Chemicon, MAB2166, WB 1:5000), eGFP (Clontech-Living Colours, cat.No.632375, WB 1:5000), α-tubulin (Sigma Aldrich, clone DM1A, WB 1:2000), V5 epitope tag in DNAJB6b (Thermo Fisher Scientific, cat. No.R960–25, WB 1:2000, IF 1:50), NC-82 (DSHB, WB 1:5000) were used. DAPI for nuclei staining (cat.No.D1306) was from Thermo Fisher Scientific. 20%

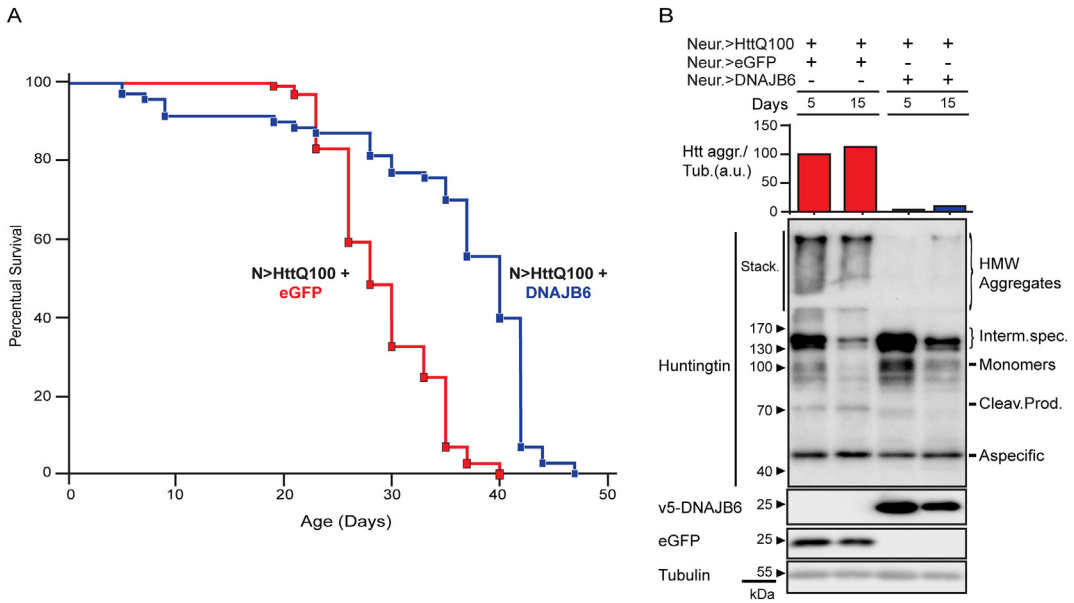

Fig. 3. Effect of neuronal DNAJB6 expression on PolyQ-HTT aggregate formation and lifespan in a pan-neuronal HttQ100-mRFP *D. melanogaster* model. A) Lifespan of isogenised male flies co-expressing neuronal (N >) HttQ100-mRFP and neuronal (N >) DNAJB6 or eGFP. Lifespan of DNAJB6-expressing line (blue curve) is significantly expanded compared to the control line (red curve). Additional control lines, comparisons, statistics and genotypes are provided in Fig. S3-1 E, G. **B)** Western Blots of total head lysates of 5 and 15-day-old adult female flies (with equal transgenes expression of flies in Fig. 3A). Anti-huntingtin antibody used for detection of monomers (100 kDa), cleaved products (70 kDa), intermediate aggregated species (130–170 kDa) and HMW aggregates (stacking gel) of HttQ100-mRFP. Anti-V5 antibody for (V5 tagged) DNAJB6 detection. Anti-GFP antibody for eGFP detection. Tubulin was used as loading control. HMW aggregates of HttQ100-mRFP quantification (signal in stacking gel normalized on tubulin signal; a.u.: arbitrary units) for each line is shown. Number of fly heads per each lysate sample and genotypes in Materials and Methods. An independent repeat of the experiment is shown in Fig. S3-1H. (For interpretation of the references to colour in this figure legend, the reader is referred to the web version of this article.)

SDS Solution (cat.No.1610418) was from BioRad. PBS components (NaCl cat.No.S9888, KCl cat.No.P9541, Na2HPO4 cat.No.255793, KH2PO4 cat.No.V000225), Tween-20 (cat.No.P2287), Triton X-100 (cat.No.T8787), Bovine Serum Albumin (cat.No.A2058, BSA), glycerol (cat.No.G5516), 3.7% Formaldehyde (cat.No.11–0705 SAJ), Tris base (cat.No.T1503) and β-mercaptoethanol (cat.No.M6250) were from Sigma Aldrich.

2.5. *D. melanogaster stocks maintenance*

All stocks and experimental flies were kept in polystyrene vials 25 × 95 mm filled with 8 ml/vial of solidified media (17 g/l Agar; 26 g/l Yeast; 54 g/l Sugar; 1.3 mg/l Nipagin). All experimental flies were maintained in a humidified and temperature controlled incubator at 25 °C on a 12 h' light and 12 h' dark cycle (Premium ICH Insect Chamber, Snijders Labs). Experimental flies, anesthetized on a CO2 pad, were selected according to their gender and phenotype by light microscope visualization.

2.6. *Lifespan curves*

Parental flies (5–6 females and 5–6 males) were kept in vial for 3 days and then removed. Offspring virgin flies were collected in the same 24 h. For each analysed group, ≈100 flies of specific gender and phenotype were collected and kept in new vials (10 flies/vial). Flies were transferred to new vials containing fresh medium every 2 days and deaths were scored daily. Statistical significance of curves differences analysed with Log rank (Mantel-Cox) test (test 1) and Gehan-Breslow-Wilcoxon test (test 2) using Graph Pad Prism Software Version 5.00. All curves comparisons were made from flies analysed in the same experiment. T50 was defined as the time point at which 50% of the initial population has died.

2.7. *Western Blotting D. melanogaster total head lysates preparation*

30–40 *D. melanogaster* adults with specific phenotype, gender, age (days after pupal eclosion) and condition were collected; after freezing in liquid nitrogen and vortexing of entire flies, separated heads were collected, counted and lysed in SDS-rich buffer (SDS 1.45%, Glycerol 20%; Tris Base 0.2 M. 2.5 µl of buffer/head) using sonication (3 pulses of 50 W for 5 s). Homogenized lysate was then centrifuged at 1000 x g for 3 s to separate cuticle debris from supernatant. Proteins in supernatant were collected and quantified using spectrophotometry (Implant NanoPhotometer UV/Vis). Protein content was equalized. Samples, supplied with β-mercaptoethanol 5% and bromophenol blue, were boiled at 99 °C for 5 min. Equal amounts of volume were resolved on SDS-PAGE. Flies of the same line were collected from different vials and the entire experiment was repeated at least 2 times.

2.8. *Western Blotting and Blot quantification*

Following the preparation of samples, proteins were resolved by SDS-PAGE, transferred to nitrocellulose membrane and processed for Western Blotting. Primary antibodies (at concentrations mentioned above) were prepared in 3% BSA/PBS-Tween 20 0.1%, secondary antibodies at concentration 1:5000 (Invitrogen, horse peroxidase conjugated to IGG or IGM) in 5% milk/PBS-Tween 20 0.1%. For visualization membranes were incubated with Pierce ECL Western Blotting substrate (cat. No. 32106) for 2 min and visualized using ChemiDoc Touch Imaging System (BioRad). Blots have been quantified using Image Lab Version 5.2.1 software (BioRad).

2.9. *Imaging of fluorescent eyes in D.melanogaster and quantification*

Experimental *D. melanogaster* adults with specific phenotype, gender, age (days after pupal eclosion) and condition were kept anesthetized on a CO2 pad and their GFP fluorescent eyes were visualized

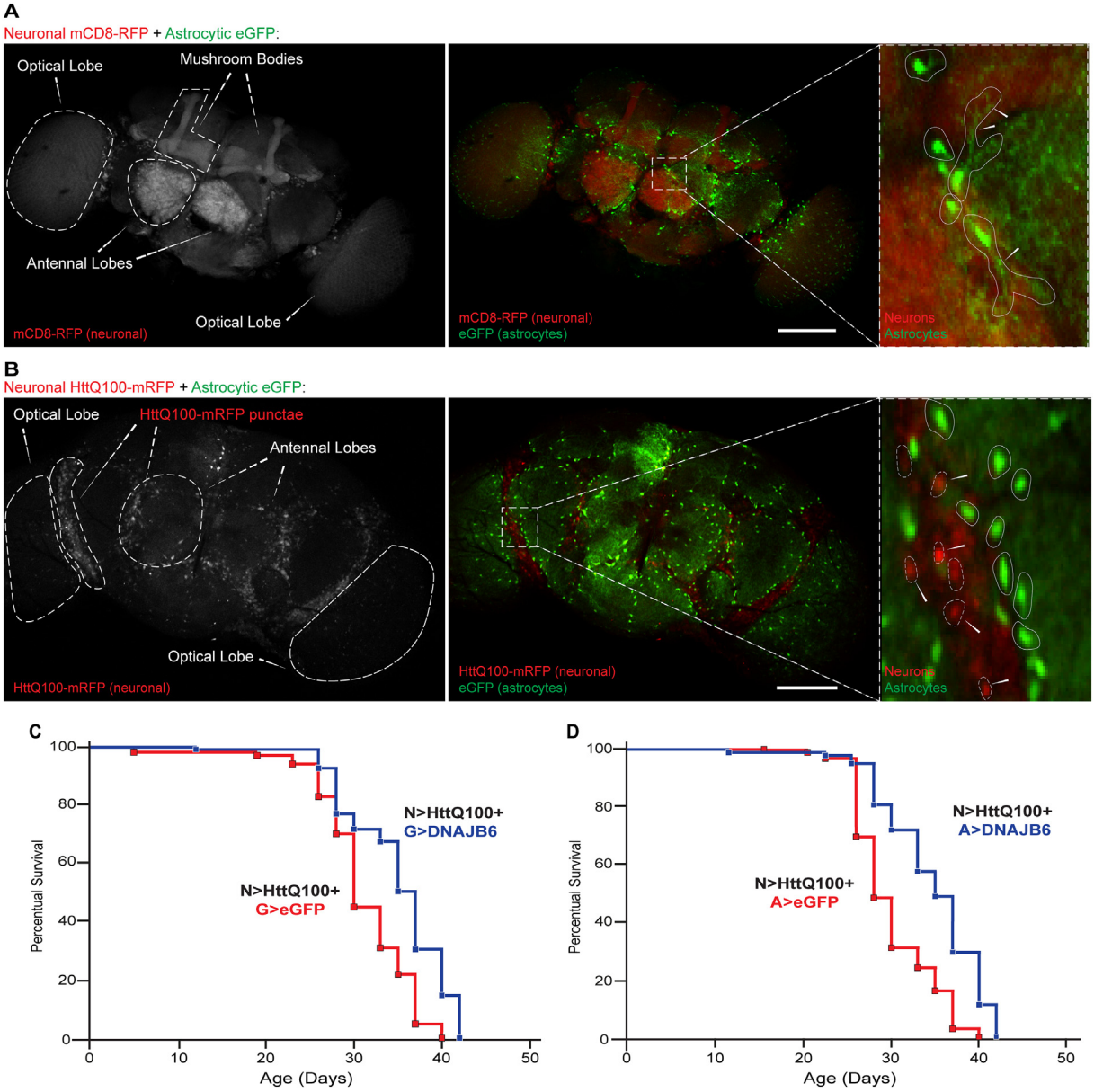

Fig. 4. Effects of glial or astrocytic DNAJB6 expression on lifespan in a pan-neuronal HttQ100-mRFP *D. melanogaster* model. A,B) Representative confocal images of brains from 15-day-old adult male flies co-expressing transgenes in different cell types using the two independent expression systems: mCD8-RFP (Fig. 4A) or HttQ100-mRFP (Fig. 4B) in all neurons and eGFP in astrocytes. Neuronal lobes and regions rich of HttQ100-mRFP punctae are shown. In the detail of the merged image of Fig. 4A, astrocytes (closed circles) with their processes (arrows) are indicated. In the detail of the merged image of Fig. 4B, neurons bodies (dashed circles) with HttQ100-mRFP punctae (arrows) and astrocytes (closed circles) are indicated. Scale bar: 100 μm. Magnification: 20×. Genotypes in Materials and Methods. **C, D)** Lifespan of isogenised male flies co-expressing neuronal (N >) HttQ100-mRFP with either glial (G >) DNAJB6 or eGFP (Fig. 4C) or astrocytic (A >) DNAJB6 or eGFP (Fig. 4D). Lifespan of DNAJB6-expressing line (blue curve) is significantly expanded compared to the control line (red curve) both for Fig.4C and Fig.4D. Additional control lines, comparisons, statistics and genotypes are provided in Fig. S4-1 B,C and F. (For interpretation of the references to colour in this figure legend, the reader is referred to the web version of this article.)

using Leica MZ10 F Fluorescence stereomicroscope (GFP3 filter). 10 eyes of different flies / group were visualized and GFP fluorescence was quantified using Image J 1.48v software and expressed as corrected mean eye fluorescence (CMEF). CMEF has been calculated as: Integrated Density - (Selected Area x Mean Background Fluorescence). Statistical significance of CMEF differences analysed with 1-way ANOVA test using Graph Pad Prism Software Version 5.00.

2.10. Analysis of eye degeneration at light microscope

For each condition, at least 80 fly eyes were checked. The fraction of the eyes that showed degeneration phenotype were calculated as previously (Vos et al., 2010). For each analysed line, eyes of at least 40 flies were scored. The results were average of at least three independent experiments.

2.11. D.melanogaster Immunofluorescence (IF), Imaging and Punctae Quantification

Brains of experimental *D. melanogaster* adults with specific phenotype, gender, age (days after pupal eclosion) and condition were dissected by light microscope visualization, in 0.1% Triton X-100 PBS 1× buffer and then fixed in 3.7% Formaldehyde, 0.1% Triton X-100 PBS 1× buffer for 20 min at room temperature. Staining of brains was

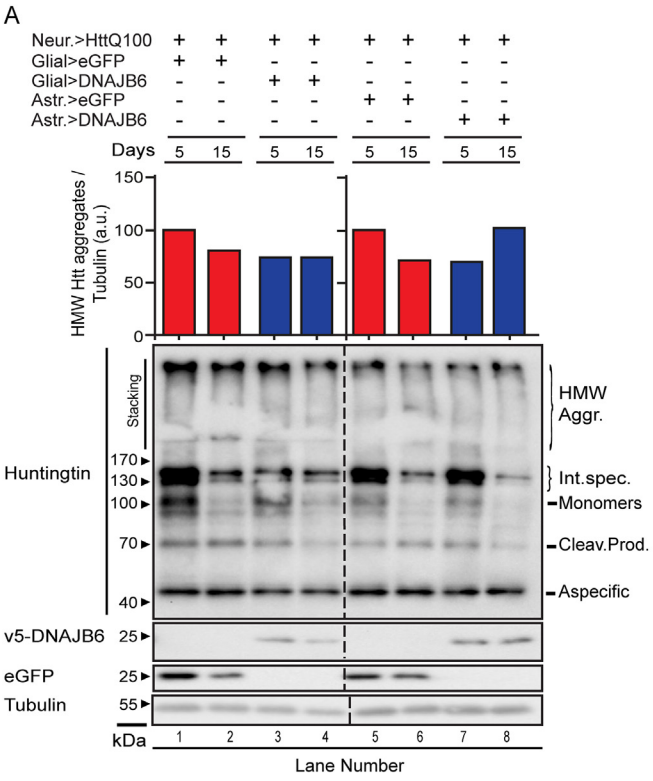

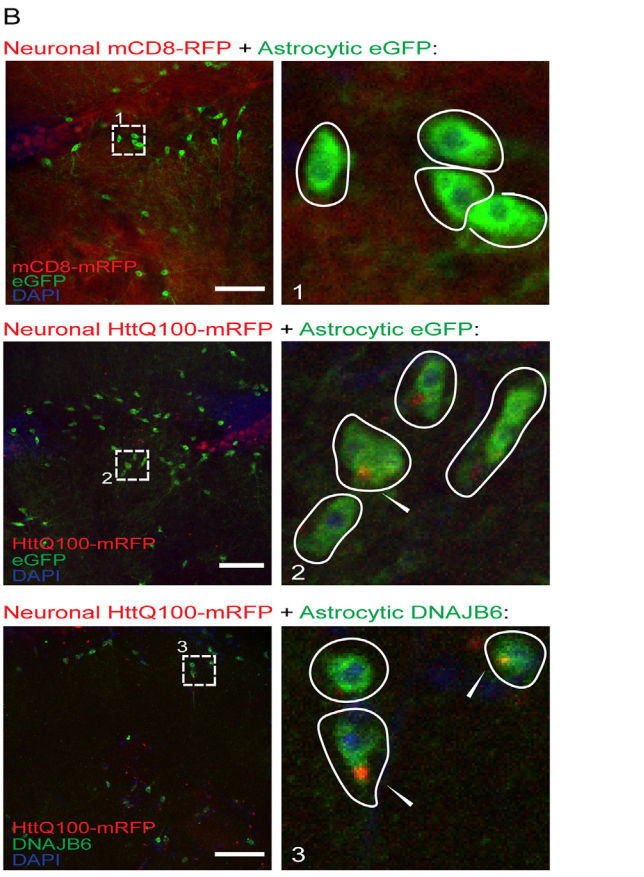

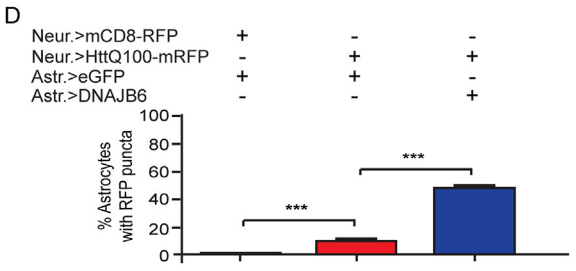

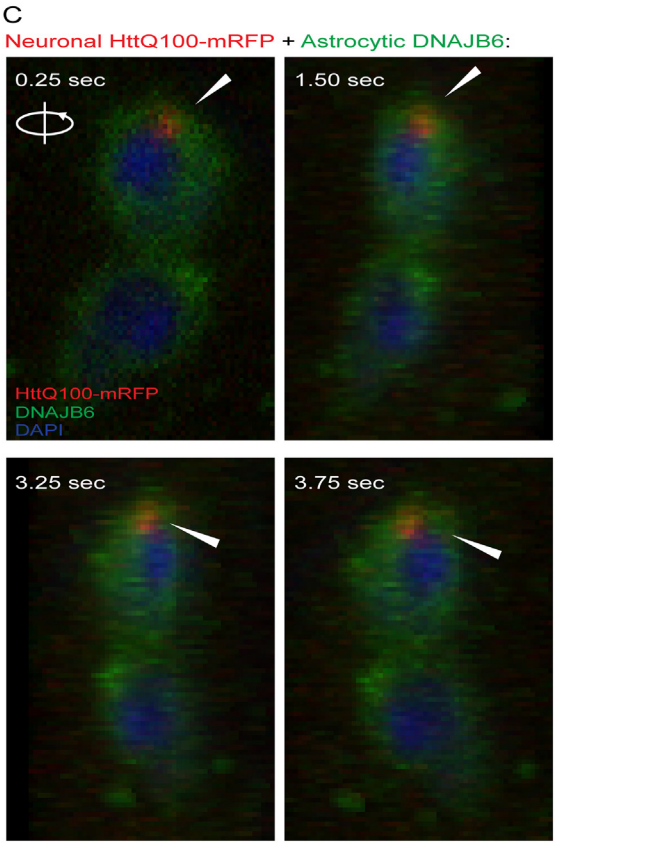

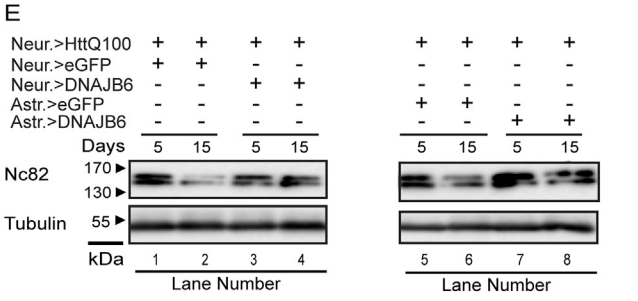

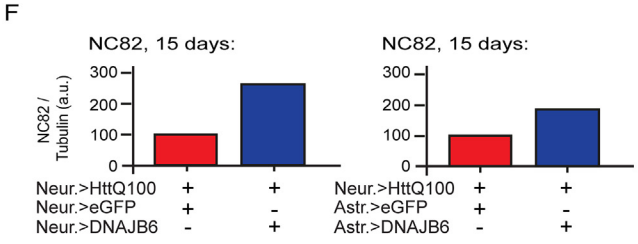

(caption on next page)

Fig. 5. Effect of glial or astrocytic DNAJB6 expression in the pan-neuronal HttQ100-mRFP *D. melanogaster* model on aggregates formation, aggregate distribution within the brain and overall neuronal fitness. A) Western Blots of total head lysates of 5 and 15-day-old adult female flies co-expressing neuronal (Neur. >) HttQ100-mRFP and glial (Glial > , lines 1–4) or astrocytic (Astr. > , lines 5–8) DNAJB6 or eGFP. Anti-huntingtin antibody used for detection of monomers (100 kDa), cleaved products (70 kDa), intermediate aggregated species (130–170 kDa) and HMW aggregates (stacking gel) of HttQ100-mRFP. Anti-V5 antibody for (V5 tagged) DNAJB6 detection. Anti-GFP antibody for eGFP detection. Tubulin was used as loading control. HMW aggregates of HttQ100-mRFP quantification (signal in stacking gel normalized on tubulin signal; a.u.: arbitrary units) for each line is shown. Number of fly heads per each lysate sample and genotypes in Materials and Methods. An independent repeat of the experiment is shown in Fig. S5-1B. **B)** Representative confocal images of brains from 15-day-old adult male flies co-expressing neuronal mCD8-RFP or HttQ100-mRFP and astrocytic DNAJB6b or eGFP. For each indicated condition, a representative picture of the region in central brain indicated in Fig. S5-1D is shown. In panels 1–3, detailed images are provided showing astrocytes (closed circles) and HttQ100-mRFP punctae in astrocytes (arrows), used for the counting in Fig. 5D. Anti-V5 antibody and Alexa488 secondary antibody were used for (V5 tagged) DNAJB6 detection. Scale bar: 25 μm. Magnification: 40×. Genotypes in Materials and Methods. **C)** Frames from the representative Movie M1 (3D confocal image reconstruction) at different time points, showing astrocytes expressing DNAJB6b and containing HttQ100-mRFP puncta (arrows) from 15-day-old adult male flies expressing the indicated transgenes. Frames show the same cells from different angles. Anti-V5 antibody and Alexa488 secondary antibody were used for (V5 tagged) DNAJB6 detection. Magnification: 63×. Genotypes in Materials and Methods. **D)** Percentage of green fluorescent astrocytes containing HttQ100-mRFP puncta in a confocal section of brains from flies of Fig. 5B and Fig. S5-1E (2 brains, 20 sections per condition). Statistical significance analysed with 1-way ANOVA test (SEM, ***, $p < 0{,}001$). **E)** Western blots of NC82 from total head lysates of 5 and 15-day-old adult female flies co-expressing neuronal (Neur. >) HttQ100-mRFP and neuronal (Neur. >) or astrocytic (Astr. >) DNAJB6 or eGFP. Anti-NC82 antibody for NC82. Tubulin was used as loading control. Number of fly heads per each lysate sample and genotypes in Materials and Methods. An independent repeat of the experiment is shown in Fig. S5-1H. **F)** Quantification of NC82 of data in Fig. 5E at day 15 (signal normalized on tubulin; a.u.: arbitrary units). (For interpretation of the references to colour in this figure legend, the reader is referred to the web version of this article.)

performed by blocking not specific sites using 2% BSA, 0.1% Triton X-100 PBS 1× buffer for 30 min at room temperature, then incubating with primary antibody (dilution 1:50) in blocking buffer for 2 days at 4 °C and finally with secondary Alexa-conjugated dyes antibody (Invitrogen, Alexa Fluor 488 goat-anti-mouse; dilution 1:500) and DAPI (final concentration 0.2 μg/μl) in blocking buffer for 2 days at 4 °C, to respectively visualize primary antibodies and nuclei. Brains were mounted between glass slide and coverslip, embedded in mountant solution (CitiFluor, Agar Scientific) and visualized by confocal microscopy within 24 h. IF images of D.melanogaster brains were captured using confocal laser scanning microscope (Leica TCS SP8). *Z*-stack images were obtained to check for the punctae in cells at different Z-planes. Quantification of the punctae in cells was carried out manually. Photoshop, and Image J software were used for image processing and to generate the 3D reconstruction (Supplementary Movie M1). Statistical significance of values differences analysed with 1-way ANOVA test using Graph Pad Prism Software Version 5.00.

3. Results

In order to test whether and how the expression of HSPs in astrocytes might be relevant for neuroprotection in PolyQ diseases, we decided to use DNAJB6, one of the most potent human chaperones in providing protection against these diseases in different in vitro and in vivo models (Hageman et al., 2010; Kakkar et al., 2016b).

We first verified whether this protective function of human DNAJB6 against PolyQ aggregation was also maintained in *D. melanogaster*. To do so, we first used the ommatidia integrity of transgenic *D. melanogaster* lines as readout for PolyQ-mediated degeneration. Hereto, the construct HttQ100-mRFP (encoding for human PolyQ-HTT exons 1–12; Weiss et al., 2012) was expressed in fly ommatidia together with human DNAJB6 (short nuclear and cytosolic isoform B; Hanai and Mashima, 2003) and the membrane-targeted mCD8-GFP (a quantifiable fluorescent reporter of internal ommatidia integrity, established and validated in different *D.melanogaster* ommatidia-models of PolyQ diseases; Burr et al., 2014), using the *gmr* promoter driven by the Gal4-UAS expression system (Brand and Perrimon, 1993). The sole expression of HttQ100-mRFP caused a significant reduction in mCD8-GFP fluorescence in ommatidia (Fig. 1A, B) and in total mCD8-GFP protein levels (Fig. 1C, D), indicating the degeneration of ommatidia. Both endpoints were alleviated by co-expression of DNAJB6 in the same cells (Fig. 1A-D), which implies a cell-autonomous protective effect of this HSP against HttQ100-mRFP toxicity. Notably, HttQ100-mRFP aggregation and mCD8-GFP levels are inversely correlated, further validating the use of this reporter, and confirming previous mechanistic findings that DNAJB6 can directly prevent the aggregation of PolyQ proteins in a cell-autonomous manner (Hageman et al., 2010; Kakkar et al., 2016b). Comparable data were found when *co*-expressing DNAJB6 with a truncated ataxin-3 (ATXN3) carrying an expanded PolyQ (ATXN3-Q78) (Warrick et al., 1998), responsible for spinocerebellar ataxia type 3 (OMIM:#109150) (Costa and Paulson, 2012) (Fig. S1-1A). This confirms our previous findings that the protective action of DNAJB6 is generic for the core PolyQ-expansion (Månsson et al., 2014) and independent from regions flanking the PolyQ expansion for which it is known that they can affect the aggregation propensity of the PolyQ-containing protein (Kuiper et al., 2017). In line with the protective action against cell degeneration, DNAJB6 expression also resulted in a reduction in the amount of HttQ100-mRFP aggregates in total head lysates (Fig. 1C, D).

Next, we generated a *D. melanogaster* line expressing HttQ100-mRFP in all neurons using the validated and well-characterized pan-neuronal promoter *elav*-Gal4 (Yao et al., 1993). Western blots of total head lysates showed abundant levels of HTT monomers, cleaved products, aggregating intermediates and high molecular weight (HMW) HTT-aggregates in 5-day-old adult male (Fig. 2A) and female (Fig. S2-1A) flies. In 15-day-old adults, monomers and other intermediate species were remarkably decreased and HMW aggregates were still present, indicating progressive aggregation and a worsening of the HD-phenotype. Lifespan analysis showed a significant reduction in lifespan of HttQ100-mRFP expressing males (Fig. 2B), with a T50 decrease of 55% (Fig. S2-1B; a comparable effect has been also observed in females, data not shown).

Subsequently, we used the GAL4-UAS and LexA-LexO (Yagi et al., 2010) expression systems that can drive expression of transgenes in a completely independent and non-overlapping manner (Fig. S3-1A-D). We generated lines co-expressing HttQ100-mRFP regulated by GAL4-UAS and DNAJB6 by LexA-LexO, solely in neurons (using the *elav* promoter). Neuronal expression of DNAJB6 extended the lifespan of flies co-expressing neuronal HttQ100-mRFP, increasing the T50 by 43% (Fig. 3A, Fig. S3-1G). The line co-expressing neuronal eGFP and HttQ100-mRFP showed a lifespan comparable to that of flies expressing neuronal HttQ100-mRFP only (compare Fig. 2B, Fig. S2-1B with Fig. 3A, Fig. S3-1E, G). This indicates that combined use of multiple promoters and eGFP expression was without any biological consequences, meaning that the lifespan reduction in the line co-expressing neuronal eGFP and HttQ100-mRFP of Fig. 3A is primarily due to the expression of the toxic PolyQ protein. Expression of DNAJB6 in neurons of control flies did not result in lifespan modulating effects (Fig. S3-1F, G), indicating that the protection in the PolyQ model is not due to a non-specific fitness-enhancing effect of DNAJB6. Again, in line with the previous observations (Hageman et al., 2010; Kakkar et al., 2016b) and the data on *D.melanogaster* eyes-degeneration (Fig. 1), we found that

neuronal expression of DNAJB6 also reduced the amount of HttQ100-mRFP aggregates in total head lysates (Fig. 3B, Fig. S3-1H). Together these data imply and confirm that DNAJB6 has a specific and cell-autonomous protective activity against HttQ100-mRFP mediated toxicity in neurons that is associated with its ability to reduce PolyQ aggregate formation (Månsson et al., 2014). Notably, brain cell degeneration due to HttQ100-mRFP toxicity might lead to reduce expression of the various transgenes during the time and disease progression, but this does not change the overall conclusion of the above described experiments.

Astrocytes have been suggested to play a key role in many aggregate-related NDs, including HD (Sofroniew and Vinters, 2010; Ben Haim et al., 2015). On the one hand, it has been suggested that the neuronal damage leads to astrocyte reactivity, which compromises their functions in nourishing and protecting neurons. On the other hand, data from rodent HD models and indirect evidence derived from human HD brains (Jansen et al., 2016) suggested that PolyQ-HTT may also be directly toxic to astrocytes, thus contributing to their chronic reactivity and to a neurodegenerative phenotype. In line with these findings and those from rodent models expressing PolyQ-HTT in astrocytes (Shin et al., 2005; Bradford et al., 2009), we observed that the selective expression of HttQ100-mRFP in the astrocytes of *D. melanogaster* (using the validated and characterized astrocyte-specific *alrm*-Gal4 promoter; Doherty et al., 2009) reduced the lifespan of the cohort (Fig. S4-1A, F).

Astrocytes are generally considered to be more resistant to PolyQ-HTT aggregation and toxicity than neurons (Jansen et al., 2014; Jansen et al., 2016) and hence PolyQ diseases are primarily thought to be due to neuronal dysfunction and death. Moreover, although chronic astrocyte reactivity is considered to be detrimental, the initial astrocytic responses have been suggested to actually counteract the progression of neurodegeneration. However, direct evidence to substantiate this hypothesis is lacking. Importantly, altered expression of several HSPs in astrocytes are amongst such molecular changes (Durrenberger et al., 2009; Seidel et al., 2012; Wilhelmus et al., 2006; Dabir et al., 2004), the relevance of which has not been demonstrated so far.

Having established that the neuronal cell-autonomous protection of human DNAJB6 is recapitulated in the *D.melanogaster* system, we addressed whether the up-regulation of chaperones, like DNAJB6, in astrocytes might non-cell autonomously protect neurons against PolyQ mediated degeneration. To test this hypothesis, we selectively expressed DNAJB6 in astrocytes (using the specific promoter *alrm*-LexA; Doherty et al., 2009), or in all glial cells (using the pan-glial promoter *repo*-LexA; Xiong et al., 1994), in the flies co-expressing HttQ100-mRFP in neurons (Fig. S3-1A-D and Fig. 4). Whereas PolyQ-HTT is ubiquitously expressed in HD human brains and rodent models of HD like R6/2 mice, in our fly model the PolyQ protein, HttQ100-mRFP, is exclusively expressed in neurons, but not in astrocytes or glial cells (Fig. 4): this enabled us to exclusively investigate whether astrocytic/glial DNAJB6 expression might exert non-cell autonomous protective effects against the toxicity mediated by the PolyQ proteins expressed in neurons. The tissue specific-expression via each of these promoters was confirmed by confocal microscopic analysis: control brains with mCD8-RFP in neurons and eGFP in astrocytes show non-overlapping staining as evidenced by diffuse mCD8-RFP fluorescence in neuronal lobes (e.g. antennal lobes, mushroom bodies), surrounded by a network of eGFP-positive astrocytes with ramified processes (Fig. 4A). Staining of brains of flies expressing neuronal HttQ100-mRFP was slightly lower. HttQ100-mRFP foci reminiscent of aggregate formation, were mainly detected in the neurons (Fig. 4B).

Strikingly, the exclusive expression of DNAJB6 in all glial cells significantly expanded the lifespan of flies expressing pan-neuronal HttQ100-mRFP, increasing the T50 by 23% (Fig. 4C, Fig. S4-1B, F). In fact, the exclusive expression of DNAJB6 in astrocytes only resulted in a similar lifespan extension in flies expressing pan-neuronal HttQ100-mRFP (25%, Fig. 4D, Fig. S4-1C, F), indicating that the expression of DNAJB6 in this specific type of glial cells alone suffices to provide non-cell autonomous protection against PolyQ mediated toxicity. The lifespan extension in these lines is also not as pronounced as observed when DNAJB6 is expressed in neurons (in which T50 is increased by 43%; Fig. 3A, Fig. S3-1G), suggesting that the pro-survival mechanisms mediated by DNAJB6 expression in different cell types might be mechanistically distinct and not completely equal in terms of effectiveness. Similar to what we found for exclusive DNAJB6 expression in neurons, DNAJB6 expression in all glial cells (Fig. S4-1D, F) or astrocytes (Fig. S4-1E, F) did not affect lifespan in control flies, indicating its specific effect on HttQ100-mRFP related toxicity. In a similar approach, we also found that DNAJB6 expression in astrocytes alleviated the level of eye degeneration caused by expression of ATXN3-Q78 in fly ommatidia (Fig. S1-1B).

In order to investigate the mechanism underlying this non-cell autonomous protection, we first considered the possibility of intercellular transmission of DNAJB6 from glial cells to neurons (Takeuchi et al., 2015) (Fig. S5-1A). For this hypothesis to be true, such a transfer should lead to reduced aggregation of HttQ100-mRFP, similar to what we observed for the cell-autonomous protection via the expression of DNAJB6 in neurons (Fig. 3B, Fig. S3-1H). However, DNAJB6 expression in all glial cells or astrocytes was not associated with a comparable dramatic reduction of HMW HttQ100-mRFP aggregates in total head lysates (Fig. 5A, Fig. S5-1B). These data confirm the specificity of the used expression systems. More importantly, these data imply that the intercellular glia-to-neurons transmission of DNAJB6 is unlikely the only or the dominant mechanism for the non-cell autonomous protective effects of DNAJB6 on the lifespan of neuronal HttQ100-mRFP flies.

In view of these results, we next investigated if other additional pro-survival and non-cell autonomous mechanisms would take place when DNAJB6 is expressed in astrocytes. It has been suggested that PolyQ-HTT aggregates may spread throughout the brain in a prion-like manner (Brundin et al., 2010; Costanzo and Zurzolo, 2013; Ren et al., 2009; Babcock and Ganetzky, 2015) (Fig. S5-1C) and that this progressive spread of disease-associated proteins contributes to the progression of the neurodegenerative process. In theory, astrocytes might restrict such spreading via actively taking up prion-like protein species, a capacity that might be limited by the progressive accumulation of toxic aggregates (Pearce et al., 2015) (Fig. S5-1C). In line with this idea, confocal microscopic analysis of flies co-expressing neuronal HttQ100-mRFP and astrocytic eGFP, revealed that approximately ~10% of eGFP-expressing astrocytes, contained mRFP punctae (Fig. 5B, D; Fig. S5-1D, S5-1E). These puncta are reminiscent of protein aggregation and under all conditions are qualitatively associated with the relative amounts of insoluble proteinaceous material detected in our western analyses. This phenomenon was not due to indiscriminate protein transfer, as shown by the absence of mRFP punctae in eGFP astrocytes of the control line expressing neuronal non-aggregating membrane-bound mCD8-RFP (Fig. 5B, D; Fig. 5D, E). These data support the hypothesis that PolyQ HTT aggregates can indeed be transferred from neurons to astrocytes. Importantly, the combined expression of neuronal HttQ100-mRFP with astrocytic DNAJB6 resulted in a significant increase in the frequency of astrocytes with RFP punctae to ~50% (Fig. 5B-D; Fig. S5-1D, S5-1E), suggesting that DNAJB6 expression positively influenced the capacity of astrocytes of taking up such prion-like species (Fig. S5-1C). 3-D confocal analyses confirmed that HttQ100-mRFP aggregates are indeed inside astrocytes (Fig. 5C, Supplementary Movie M1).To confirm that the expression of astrocytic DNAJB6 indeed resulted in the actual and specific non-cell autonomous protection of neurons, we analysed the level of the neuronal marker NC82 (Wagh et al., 2006) in total fly head lysates. NC82 (Bruchpilot) is a key synaptic protein for the activity and integrity of the pre-synaptic zone in *D.melanogaster* brain (Wagh et al., 2006). NC82 is critical for a normal-evoked neurotransmitter release at the chemical synapses and, notably, the RNAi-induced-reduction of neuronal NC82 expression leads to an alteration of the normal synaptic components, to locomotor inactivity, and to unstable flight in adult *D.melanogaster* (Wagh et al., 2006). The expression level of NC82 provides therefore a direct measure of the functional fitness of the neuronal

population. We found NC82 levels to be strongly decreased in 15-day-old flies solely expressing neuronal HttQ100-mRFP (Fig. S5-1F, G). This NC82-decline was not only alleviated in flies co-expressing neuronal DNAJB6 (cell autonomous protection), but also in flies co-expressing DNAJB6 in astrocytes (non-cell autonomous protection, Fig. 5E, F, Fig. S5-1H, I), implying an overall improvement of overall neuronal fitness in both cases.

4. Discussion

Our data are a direct demonstration of a long-assumed hypothesis that glial cells, and particular astrocytes, might play a modulating role in HD, which as in many other NDs, initially and primarily affects neurons.

PolyQ-HTT is expressed in glial cells in the brain of HD patients and animal models (Jansen et al., 2016). In line with previous data from rodent models (Shin et al., 2005; Bradford et al., 2009), we confirmed that PolyQ-Htt exclusively expressed in astrocytes reduces lifespan in *D.melanogaster*. These data thus indicate that astrocytic PolyQ-HTT may contribute to HD pathology and that astrocytic damage is generally detrimental to the health of the brain, as notably observed in Alexander disease (OMIM:#203450), a genetic neurodegenerative disorder that primarily affects astrocytes by a dominant gain-of-function mutation of the *GFAP* gene (Sofroniew and Vinters, 2010; Olabarria and Goldman, 2017).

However, our data revealing neuroprotection by expression of DNAJB6 in astrocytes differ from these latter studies (Jansen et al., 2016; Shin et al., 2005; Bradford et al., 2009), as astrocytes in our *D. melanogaster* model do not express PolyQ-HTT. Still, we found that DNAJB6-expressing astrocytes provide a non-cell autonomous protective effects against degeneration of neurons expressing PolyQ-HTT. Thus, these data for the first time reveal that astrocytes empowered with sufficient chaperone activity, provided by DNAJB6, can provide protection against degeneration of neurons in HD.

DNAJB6, the chaperone used in this study, has cell-autonomous protective effects as previously shown (Kakkar et al., 2016b), which are strongly associated with its ability to prevent the initiation of PolyQ aggregation by the core-polyQ fragment, irrespective of regions flanking the expansion (Hageman et al., 2010; Månsson et al., 2014), for which it is known that they can affect the aggregation propensity of the PolyQ-containing protein (Kuiper et al., 2017). Our findings for both in vivo PolyQ HTT and PolyQ ATXN3 fly models show that also not only the cell autonomous, but also the non-cell autonomous effects of DNAJB6 are generic for PolyQ proteins.

Interestingly, the non-cell autonomous protection evoked by DNAJB6 expression in astrocytes is not associated with a reduction in PolyQ-HTT aggregation. Although it has been suggested that DNAJs and other HSPs can be transmitted between cells via exosomes (Takeuchi et al., 2015), the absence of an effect on total aggregate formation in our study implies that additional mechanisms may underlie the DNAJB6-mediated non-cell autonomous protection.

Despite the use of well-established promoters and two independent expression systems, it could still be argued that low levels of neuronal DNAJB6, due to an eventual leakage of the *repo*-LexA and *alrm*-LexA promoters and beyond detection limit of our microscopic analyses, could have been responsible for the observed protection evoked by DNAJB6 expression in astrocytes. However, using a weaker *elav* promoter to drive neuronal DNAJB6 expression than those used in the presented data (i.e. using the *elav*-LG instead of the *elav*-LhG promoter (Fig. S3-1A-D and Yagi et al., 2010)) we found no significant cell autonomous protection, whereas we could still detect neuronal DNAJB6 expression (data not shown). This implies that it is highly unlikely that the observed protection by astrocytic DNAJB6 expression is due to leakage of the *repo*-LexA and *alrm*-LexA promoters.

This implies that the observed non-cell autonomous protection via astrocytic DNAJB6 expression is directly due to an activity of the chaperone in the astrocytes enhancing its fitness and function. We hypothesize such may delay the trans-cellular spreading of PolyQ HTT aggregates in the *D.melanogaster* brain. Cellular experiments have indeed demonstrated that PolyQ-HTT aggregates can enter cells where they can initiate intracellular seeding (Kakkar et al., 2016b; Ren et al., 2009) and can spread between neurons in the *D.melanogaster* brain (Babcock and Ganetzky, 2015). Our data show that, in the same organismal system, these neuronal PolyQ-HTT aggregates can end up in astrocytes in agreement with observations by Pearce and colleagues (Pearce et al., 2015), using axotomised neurons. The uptake of neuron-derived aggregates could imply that astrocytes act as a “reservoir” for these toxic prion-like species, thereby preventing their neuron-to-neuron spreading in the brain and hence delaying the progression of neurodegeneration. The prion-reservoir capacity of astrocytes is likely limited by the toxicity of captured aggregates. However, the upregulation of chaperones like DNAJB6 may enhance this capacity, which is supported by our data showing that the frequency of astrocytes with inclusions is increased in case of DNAJB6 overexpression. This provokes the speculation that DNAJB6 can positively influence the prion-reservoir capacity of astrocytes and their ability to prevent the spreading of prion-like species in the brain, via its protective functions against PolyQ-HTT toxicity (Hageman et al., 2010). The increased prion-reservoir capacity of astrocytes ultimately results in an improvement of overall neuronal fitness and in an increased lifespan of PolyQ-HTT *D.melanogaster* model (Fig. S5-1C).

An alteration in neuroinflammation could be an additional contributor to the enhanced neuroprotection due to the DNAJB6 expression in astrocytes, which hereby might promote a more neuroprotective or less neurotoxic pathway. Indeed, astrocytic activation has been claimed to have both positive and negative effects on the progression of PolyQ diseases (Sofroniew and Vinters, 2010).

In conclusion, our findings support the hypothesis that increasing astrocyte fitness and functions by chaperones like DNAJB6 (tentatively by increasing their prion-reservoir capacity) has protective significance in HD and possibly other protein aggregation-related NDs which show a pathology associated with these prion-like species such as Alzheimer's (OMIM:#104300) and Parkinson's (OMIM:#168601) (Brundin et al., 2010; Costanzo and Zurzolo, 2013).

Supplementary data to this article can be found online at https://doi.org/10.1016/j.nbd.2018.10.017.

Conflicts of interests

The authors declare no conflict of interest.

Funding

This work was supported by the Prinses Beatrix Foundation / de Nederlandse Hersenstichting (grant # F2012(1)-104).

Acknowledgments

The authors wish to thank Jeanette F. Brunsting, Wondwossen Melaku Yeshaw, Yixian Li, Serena Carra and Jean-Christophe Billeter for their helpful suggestions.

References

Babcock, D.T., Ganetzky, B., 2015. Transcellular spreading of huntingtin aggregates in the Drosophila brain. Proc. Natl. Acad. Sci. 112, 5427–5433.
Balch, W.E., Morimoto, R.I., Dillin, A., Kelly, J.W., 2008. Adapting Proteostasis for Disease intervention. Science 319, 916–920.
Ben Haim, L., Carrillo-De Sauvage, M.A., Ceyzériat, K., Escartin, C., 2015. Elusive roles for reactive astrocytes in neurodegenerative diseases. Front. Cell. Neurosci. 9, 1–27.
Bradford, J., Shin, J., Roberts, M., Wang, C.E., Li, X.J., Li, S., 2009. Expression of mutant huntingtin in mouse brain astrocytes causes age-dependent neurological symptoms. Proc. Natl. Acad. Sci. U. S. A. 106, 22480–22485.
Brand, A.H., Perrimon, N., 1993. Targeted gene expression as a means of altering cell

fates and generating dominant phenotypes. Development 118, 401–415.
Brundin, P., Melki, R., Kopito, R., 2010. Prion-like transmission of protein aggregates in neurodegenerative diseases. Nat. Rev. Mol. Cell. Biol. 11, 301–307.
Burr, A.A., Tsou, W.L., Ristic, G., Todi, S.V., 2014. Using membrane-targeted green fluorescent protein to monitor neurotoxic protein-dependent degeneration of Drosophila eyes. J. Neurosci. Res. 92, 1100–1109.
Costa, C., Paulson, H.L., 2012. Progress in Neurobiology toward understanding Machado – Joseph disease. Prog. Neurobiol. 97, 239–257.
Costanzo, M., Zurzolo, C., 2013. The cell biology of prion-like spread of protein aggregates: mechanisms and implication in neurodegeneration. Biochem. J. 452, 1–17.
Dabir, D.V., Trojanowski, J.Q., Richter-Landsberg, C., Lee, V.M.-Y., Forman, M.S., 2004. Expression of the small heat-shock protein alphaB-crystallin in tauopathies with glial pathology. Am. J. Pathol. 164, 155–166.
Doherty, J., Logan, M.A., Taşdemir, O.E., Freeman, M.R., 2009. Ensheathing glia function as phagocytes in the adult Drosophila brain. J. Neurosci. 29, 4768–4781.
Durrenberger, P.F., Filiou, M.D., Moran, L.B., Michael, G.J., Novoselov, S., Cheetham, M.E., Clark, P., Pearce, R.K., Graeber, M.B., 2009. DnaJB6 is present in the core of Lewy bodies and is highly up-regulated in Parkinsonian astrocytes. J. Neurosci. Res. 87, 238–245.
Gillis, J., Schipper-Krom, S., Juenemann, K., Gruber, A., Coolen, S., van den Nieuwendijk, R., et al., 2013. The DNAJB6 and DNAJB8 protein chaperones prevent intracellular aggregation of polyglutamine peptides. J. Biol. Chem. 288 (24), 17225–17237.
Hageman, J., Rujano, M.A., van Waarde, M.A., Kakkar, V., Dirks, R.P., Govorukhina, N., Oosterveld-Hut, H.M., Lubsen, N.H., Kampinga, H.H., 2010. A DNAJB Chaperone Subfamily with HDAC-Dependent Activities Suppresses toxic Protein Aggregation. Mol. Cell 37, 355–369.
Hageman, J., van Waarde, M.A., Zylicz, A., Walerych, D., Kampinga, H.H., 2011. The diverse members of the mammalian HSP70 machine show distinct chaperone-like activities. Biochem. J. 435, 127–142.
Hanai, R., Mashima, K., 2003. Characterization of two isoforms of a human DnaJ homologue, HSJ2. Mol. Biol. Rep. 30, 149–153.
Hartl, F.U., Bracher, A., Hayer-Hartl, M., 2011. Molecular chaperones in protein folding and proteostasis. Nature 475, 324–332.
Jansen, A.H.P., Reits, E.A., Hol, E.M., 2014. The ubiquitin proteasome system in glia and its role in neurodegenerative diseases. Front. Mol. Neurosci. 7, 1–14.
Jansen, A.H., van Hal, M., Op den Kelder, I.C., Meier, R.T., de Ruiter, A.A., Schut, M.H., Smith, D.L., Grit, C., Brouwer, N., Kamphuis, W., et al., 2016. Frequency of nuclear mutant huntingtin inclusion formation in neurons and glia is cell-type-specific. Glia 65, 50–61.
Kakkar, V., Meister-Broekema, M., Minoia, M., Carra, S., Kampinga, H.H., 2014. Barcoding heat shock proteins to human diseases : looking beyond the heat shock response. Dis. Model. Mech. 7, 421–434.
Kakkar, V., Kuiper, E.F.E., Pandey, A., Braakman, I., Kampinga, H.H., 2016a. Versatile members of the DNAJ family show Hsp70 dependent anti-aggregation activity on RING1 mutant parkin C289G. SciRep 6, 34830.
Kakkar, V., Månsson, C., de Mattos, E.P., Bergink, S., van der Zwaag, M., van Waarde, M.A., Kloosterhuis, N.J., Melki, R., van Cruchten, R.T., Al-Karadaghi, S., et al., 2016b. The S/T-Rich motif in the DNAJB6 Chaperone Delays Polyglutamine Aggregation and the Onset of Disease in a Mouse Model. Mol. Cell 62, 272–283.
Kampinga, H.H., Bergink, S., 2016. Heat shock proteins as potential targets for protective strategies in neurodegeneration. Lancet Neurol. 15, 748–759.
Kuiper, E.F.E., de Mattos, E.P., Jardim, L.B., Kampinga, H.H., Bergink, S., 2017. Chaperones in Polyglutamine Aggregation : beyond the Q-Stretch. Front. Neurosci. 11, 1–11.
Månsson, C., Kakkar, V., Monsellier, E., Sourigues, Y., Härmark, J., Kampinga, H.H., Melki, R., Emanuelsson, C., 2014. DNAJB6 is a peptide-binding chaperone which can suppress amyloid fibrillation of polyglutamine peptides at substoichiometric molar ratios. Cell Stress Chaperones 19, 227–239.
Månsson, C., van Cruchten, R.T.P., Weininger, U., Yang, X., Cukalevski, R., Arosio, P., 2018. Conserved S/T Residues of the Human Chaperone DNAJB6 are Required for Effective Inhibition of Aβ42 Amyloid Fibril Formation. Biochemistry 57 (32), 4891–4902.
Olabarria, M., Goldman, J.E., 2017. Disorders of Astrocytes : Alexander Disease as a Model. Annu. Rev. Pathol. 12, 131–152.
Pearce, M.M.P., Spartz, E.J., Hong, W., Luo, L., Kopito, R.R., 2015. Prion-like transmission of neuronal huntingtin aggregates to phagocytic glia in the Drosophila brain. Nat. Commun. 6, 6768.
Potter, C.J., Tasic, B., Russler, E.V., Liang, L., Luo, L., 2010. The Q System: a Repressible Binary System for Transgene Expression, Lineage Tracing, and Mosaic Analysis. Cell 141, 536–548.
Ren, P.-H., Lauckner, J.E., Kachirskaia, I., Heuser, J.E., Melki, R., Kopito, R.R., 2009. Cytoplasmic penetration and persistent infection of mammalian cells by polyglutamine aggregates. Nat. Cell Biol. 11, 219–225.
Seidel, K., Vinet, J., Dunnen, W.F.A., Brunt, E.R., Meister, M., Boncoraglio, A., Zijlstra, M.P., Boddeke, H.W., Rüb, U., Kampinga, H.H., Carra, S., 2012. The HSPB8-BAG3 chaperone complex is upregulated in astrocytes in the human brain affected by protein aggregation diseases. Neuropathol. Appl. Neurobiol. 38, 39–53.
Shin, J.Y., Fang, Z.H., Yu, Z.X., Wang, C.E., Li, S.H., Li, X.J., 2005. Expression of mutant huntingtin in glial cells contributes to neuronal excitotoxicity. J. Cell Biol. 171, 1001–1012.
Söderberg, C.A.G., Månsson, C., Bernfur, K., Rutsdottir, G., Härmark, J., Rajan, S., et al., 2018. Structural modelling of the DNAJB6 oligomeric chaperone shows a peptide-binding cleft lined with conserved S/T-residues at the dimer interface. Sci. Rep. 8 (1), 5199.
Sofroniew, M.V., 2009. Molecular dissection of reactive astrogliosis and glial scar formation. Trends Neurosci. 32, 638–647.
Sofroniew, M.V., Vinters, H.V., 2010. Astrocytes: Biology and pathology. Acta Neuropathol. 119, 7–35.
Takeuchi, T., Suzuki, M., Fujikake, N., Popiel, H.A., Kikuchi, H., Futaki, S., Wada, K., Nagai, Y., 2015. Intercellular chaperone transmission via exosomes contributes to maintenance of protein homeostasis at the organismal level. Proc. Natl. Acad. Sci. U. S. A. 112, E2497–E2506.
Vos, M.J., Zijlstra, M.P., Kanon, B., van Waarde-Verhagen, M.A., Brunt, E.R.P., Oosterveld-Hut, H.M.J., Carra, S., Sibon, O.C., Kampinga, H.H., 2010. HSPB7 is the most potent polyQ aggregation suppressor within the HSPB family of molecular chaperones. Hum. Mol. Genet. 19, 4677–4693.
Wagh, D.A., Rasse, T.M., Asan, E., Hofbauer, A., Schwenkert, I., Dürrbeck, H., Buchner, S., Dabauvalle, M.C., Schmidt, M., Qin, G., et al., 2006. Bruchpilot, a protein with homology to ELKS/CAST, is required for structural integrity and function of synaptic active zones in Drosophila. Neuron 49, 833–844.
Warrick, J.M., Paulson, H.L., Gray-Board, G.L., Bui, Q.T., Fischbeck, K.H., Pittman, R.N., Bonini, N.M., 1998. Expanded Polyglutamine Protein Forms Nuclear Inclusions and Causes Neural Degeneration in Drosophila. Cell 93, 939–949.
Weiss, K.R., Kimura, Y., Lee, W.C.M., Littleton, J.T., 2012. Huntingtin aggregation kinetics and their pathological role in a drosophila Huntington's disease model. Genetics 190, 581–600.
Wilhelmus, M.M.M., Otte-Höller, I., Wesseling, P., De Waal, R.M.W., Boelens, W.C., Verbeek, M.M., 2006. Specific association of small heat shock proteins with the pathological hallmarks of Alzheimer's disease brains. Neuropathol. Appl. Neurobiol. 32, 119–130.
Xiong, W.-C., Hideyuki, O., Patel, N.H., Blendy, J.A., Montell, C., 1994. Repo encodes a glial-specific homeo domain protein required in the Drosophila nervous system. Genes Dev. 8, 981–994.
Yagi, R., Mayer, F., Basler, K., 2010. Refined LexA transactivators and their use in combination with the Drosophila Gal4 system. Proc. Natl. Acad. Sci. U. S. A. 107, 16166–16171.
Yao, K.M., Samson, M.L., Reeves, R., White, K., 1993. Gene elav of Drosophila melanogaster: a prototype for neuronal-specific RNA binding protein gene family that is conserved in flies and humans. J. Neurobiol. 24, 723–739.